Cationic Glycopolymers with Aggregation-induced Emission (AIE) for the Killing, Imaging and Detection of Bacteria

Die Li,[†] Jing Chen,[†] Mei Hong,[†] Yan Wang,[†] David M. Haddleton,[‡*] Guang-Zhao Li[§] and Qiang Zhang[†*]

[†] Key Laboratory of New Membrane Materials, Ministry of Industry and Information Technology, School of Environmental and Biological Engineering, Nanjing University of Science and Technology, Nanjing 210094, P. R. China. Email: zhangqiang@njust.edu.cn.

[‡] Department of Chemistry, University of Warwick, CV4 7AL Gibbet Hill, UK. E-mail: d.m.haddleton@warwick.ac.uk.

[§] School of Materials Science and Engineering, Xihua University, Chengdu 610039.

KEYWORDS: Aggregation-induced emission; cationic glycopolymer; antibacterial poly(ionic liquid)s; imaging; bacterial detection.

ABSTRACT

Cationic glycopolymers with similar structures of typical poly(ionic liquid)s (PILs) were synthesized *via* the quaternization reaction of poly(4-vinyl pyridine) (P4VP) with halogen-functionalized D-mannose and tetraphenylethylene (TPE) units. Such post-polymerization modification provided PILs with aggregation-induced emission effect as well as specific carbohydrate-protein recognition with lectins such as Concanavalin A. The interactions between cationic glycopolymers and different microorganisms, including gram-positive *Staphylococcus aureus* and gram-negative *Escherichia coli*, were used for the killing, imaging and detection of bacteria. Besides, these sugar-containing PILs showed relatively low hemolysis rate due to the presence of saccharide units, which may have potential application in the field of biomaterials.

Introduction

Pathogenic microorganisms can cause environmental pollution and disease infection, which seriously damage human health.[1, 2] The rapid development of antibiotic resistance can further complicate this situation.[3, 4] As a result, various kinds of antimicrobial agents, including organic (polypeptide,[5] saccharides,[6] antimicrobial enzymes,[7] cationic organic polymers[8]) and inorganic (silver,[9] graphene[10], carbon[11]) materials, have been developed to deal with microbial resistance.[12] Recently, poly(ionic liquid)s (PILs) have aroused considerable attention that can cope with microbial drug resistance.[12-14] PILs approach bacteria through electrostatic interaction between cationic groups and negatively charged cell walls, and then insert hydrophobic fragments into cell membranes, resulting in the rupture and death of bacteria.[15, 16] Quaternary ammonium,[17] phosphonium,[18] imidazolium,[19] pyridinium,[20] piperidinium,[21] and pyrrolidinium[22] cation-based PILs have been widely applied in antibacterial materials.

PILs are often toxic to cells, which greatly limits their application in medicine.[23] However, PILs constructed from biomass-derived monomers can have good biocompatibility.[24] Saccharides such as mannose, glucose etc. are ideal candidates to improve biocompatibility, which have been used in the preparation of polymers for potential biomedical application.[25, 26] Furthermore, mannose can target *Escherichia coli* (*E. coli*) because of its specific electrostatic interaction with FimH lectin on the surface of *E. coli*.[27, 28] Therefore, designing new antibacterial PILs containing saccharides is very promising in regulating cytotoxicity and targeting bacteria.[29, 30]

The commonly used colony forming unit counting method for bacterial concentration detection is criticized because it is time-consuming and tedious.[31] Recently, fluorescence method has been used in detection, screening and imaging of bacteria due to its advantages such as fast response, high sensitivity and easy operation.[32, 33] Early in the 21st century, the concept of aggregation-induced emission (AIE) entered people's sight and became a hot spot.[34] TPE is a common AIE molecule, which emits fluorescence when its intramolecular rotation is restricted in the aggregated state.[35-37] Bacteria can be detected efficiently by fluorescence emitted from TPE gathered on bacterial surface. Wang et al. synthesized fluorescent imidazolium-based PILs, whose TPE units were introduced by anion exchange, for antibacterial and imaging simultaneously.[38]

In this work, it was our aim to design and synthesize functional PILs with both pendent saccharide units and AIE probes (Scheme 1). These sugar-containing PILs could be seen as novel cationic glycopolymers, which integrate the properties of typical PILs and glycopolymers, including the specific carbohydrate-protein recognition and the antibacterial performance. Owing to the existence of pendent TPE units, the interactions between PILs and the surface biomacromolecules of bacteria (lections etc.) could cause further aggregation of PILs, leading to AIE which could be applied to bacterial concentration detection and fluorescence imaging. Thus the functional polymers developed herein have combined the properties of AIE polymers, glycopolymers and PILs, which could be used for the killing, imaging and detection of bacteria (Scheme 1). In addition, the AIE glycopolymers have shown very good photostability and the strong fluorescence intensity did not attenuate even if it was stored without protection from sunlight for several days. Moreover, these polymeric

bactericides have demonstrated good biocompatibility with mammalian cells as shown by a low hemolysis rate towards red blood cells.

Scheme 1. Schematic representation for the detection, imaging and killing of bacteria by AIE glycopolymers.

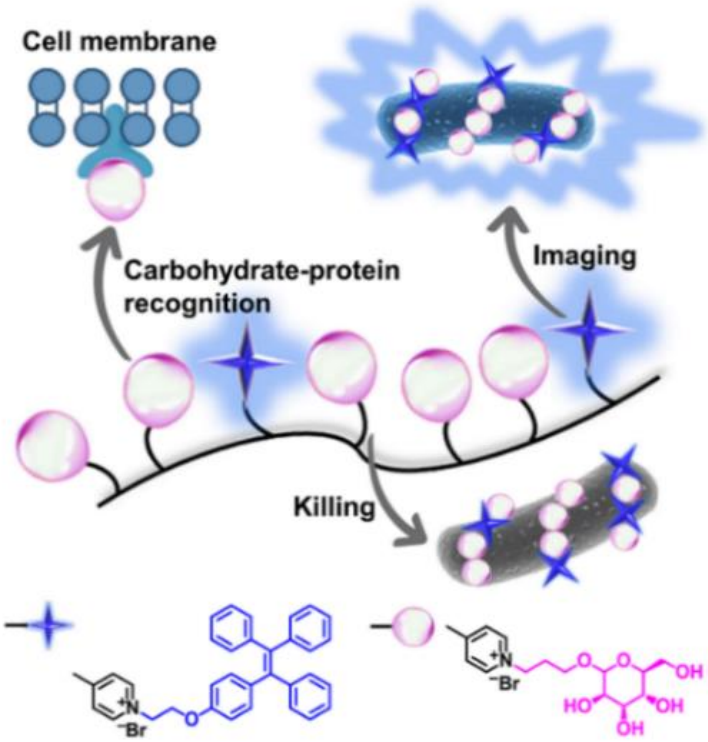

Experimental Section

Materials

Poly(4-vinylpyridine) (P4VP) was synthesized as previously.[30] Concanavalin A lectin (Con A, 95%) and 3-bromo-1-propanol (PropanolBr, 97%) were purchased from Aladdin (China). 3-Bromopropyl D-mannopyranoside (ManBr)[39] (viscous liquid) and ω-(4-tetraphenylethylene-yloxy) -1-bromoethane (TPEBr)[40] were synthesized as previously. *Staphylococcus aureus* (*S. aureus,* ATCC 6538) and *Escherichia coli* (*E. coli* ATCC 25922)

strains were obtained from Shanghai Bioresource Collection Center. Sheep blood was purchased from Nanjing Quanlong Biotech Corporation. The cutoff molecular of dialysis membrane (Spectrum Laboratories) was 1000 Da.

Instruments and analysis

^{1}H NMR spectra were measured by Bruker AVANCE III 500MHz spectrometer. Molecular weight and dispersity of P4VP were calculated by size exclusion chromatography (SEC) on Waters system using *N, N*-dimethylbenzamide (DMF, 40 ℃, 1.00 mL min^{-1}) as eluent. Zeta potential measurements were performed using Brookhaven ZetaPALS variable temperature analyzer. Fourier transform infrared (FTIR) spectra were measured by Nicolet iS5 FTIR spectrometer. The optical transmittance of solutions were acquired by Shimadzu UV-2600 spectrophotometer. The optical density (OD) of bacterial suspension was read with a microplate reader (Molecular Devices SpectraMax M3). The fluorescence intensity of solutions was measured by fluorescence spectrophotometer (Shimadzu, RF 6000). Laser scanning confocal microscopy (LSCM) was recorded using an OLYMPUS FV3000. Absolute quantum yield was measured by FLS980 Series of Fluorescence Spectrometers (Edinburgh).

Quaternization reaction of P4VP with organobromine compounds

P4VP (240 mg, ~ 2 mmol 4VP units), bromine-functionalized D-mannose (ManBr, 1204 mg, 4 mmol) or 3-bromo-1-propanol (Bromopropanol, 556 mg, 4 mmol), bromine-functionalized tetraphenylethylene (TPEBr, 91 mg, 0.2 mmol) and 10 ml of DMSO were added into a two necked round-bottomed flask. The mixture was bubbled for 15 min with N_2 and stirred at 80 °C for 5 days. Solvents and other low mass impurities were removed

by dialysis against methanol and water respectively and then lyophilized. The mannose-containing polymer product was named as P4VP-ManTPE and the bromopropanol-containing polymer as P4VP-BPTPE, whose yields were 65% and 71% respectively. As a control, cationic polymers P4VP-Man and P4VP-TPE, which did not contain TPE or mannose units, were synthesized in the same way in 77% and 30% yield respectively.

Determination of fluorescence quantum yield

Quantum yields (Φ) of PILs in aqueous solution were measured by a relative method by taking a fresh solution of quinine sulfate as standard and measuring the quantum yield with excitation wavelength at 350 nm in 0.1 mol L^{-1} H_2SO_4 being 54%.[41] In order to ensure the absorbance of quinine sulfate and PILs solution were < 0.05 below 350 nm so as to avoid the interference from self-absorption. UV/Vis was used to measure the absorbance under λ = 350 nm, and the fluorescence measured between λ = 370 nm and 600 nm with λ_{ex} = 350 nm. The relative quantum yield is calculated as follows:

$$\Phi_P = \Phi_S \frac{F_P}{F_S} \frac{A_S}{A_P}$$

where Φ means quantum yield; *A* = absorbance at λ = 350 nm; *F* is the integrated area of the peak from λ = 370 nm to 600 nm; *P* is the PILs and *S* means the standard respectively.

The absolute quantum yield of PILs in aggregation state was measured by fluorescence spectrometry at λ_{ex} = 380 nm.

Recognition between PILs and ConA

Turbidity was exploited to measure the binding ability with the lectin ConA.[42] ConA (1 mg mL^{-1}) was solubilized in HBS buffer (HEPES 2.38 g, NaCl 8.77 g, and $CaCl_2$ 0.11 g in 1 L water, pH = 7.4) and filtered through 0.2 μm nylon filters. The concentration of the ConA was calculated via the UV absorbance $\lambda < 280$ nm [Absorbance = 1.37 × [ConA] (mg mL^{-1})]. 4 mg mL^{-1} PILs solution was prepared in HBS buffer and equal volumes of PILs and ConA solutions were mixed and the absorbance was determined continuously for 3 h.

Minimum inhibitory concentration assay

The minimum inhibitory concentration (MIC) method was used to determine the antibacterial properties of P4VP-ManTPE and P4VP-BPTPE.[43] Firstly, the PILs solutions were prepared in a LB medium, and subsequently diluted 2-fold. The strains of *S. aureus* and *E. coli* were cultured in LB broth for 24 hours so as to obtain standard bacterial suspensions, and then diluted to OD_{600} (optical density, λ = 600 nm) = 1, under which case the Concentration $_{E.\ coli} \approx 0.5*10^9$ and Concentration $_{S.\ aureus} \approx 2*10^9$. The final concentration for the test was further diluted x5000. Subsequently, equal volumes of different concentrations of PILs solutions and bacterial suspension were mixed and added to 96-well plate in order to culture at 37 °C for 24 h, prior to the OD_{600} reading by a microplate reader. The MIC refers to the lowest concentration of polymers with an observed antibacterial effect.

Plate counting method to test the antibacterial activity

P4VP-ManTPE and P4VP-BPTPE were dissolved in LB broth with a concentration = 8.0

mg mL^{-1}, and diluted using a gradient method. The bacteria in LB broth (OD_{600} = 1, initial Concentration $_{E.\ coli} \approx 0.5*10^9$, Concentration $_{S.\ aureus} \approx 2*10^9$, and further diluted x5000) was co-culture with equal volume of PILs solution under different concentrations. After 1.5 h, 5 μL mixed solution was evenly coated on LB agar plate and incubated for 24 h at 37 °C, the number of bacterial colonies were recorded. The formula used for the antibacterial activity was:

$$\text{antibacterial activity } (\%) = \frac{N_{\text{negative control}} - N_{\text{sample}}}{N_{\text{negative control}}} \times 100$$

where *N* = the numbers of bacterial colonies, sample and negative control is the bacteria co-cultured with and without PILs, respectively.[38]

Morphological changes of the bacteria

The effect of the polymers on the bacteria morphology was observed by scanning electron microscopy (SEM). *S. aureus* and *E. coli* (OD_{600} = 0.2) were co-cultured with (or without) equal volume of PILs (corresponding 2*MIC concentration) in LB broth for 2 h.at 37 °C Subsequently, the bacteria were immobilized with 2.5 wt% glutaraldehyde and dehydrated using a gradient method before SEM recording.

Bacterial imaging by LSCM

A bacterial suspension was centrifuged and washed with phosphate buffer (PBS, 0.2 M, pH = 7.4), followed with dilution to OD_{600} = 0.2 with PBS. The bacterial suspension obtained was co-cultured with equal volume of P4VP-ManTPE or P4VP-BPTPE (0.2 mg mL^{-1} in PBS)

for 2 h at 37 °C, and then fixed with glutaraldehyde prior to dehydration and the treated sample used for LSCM measurement.

Detection of bacterial concentration by fluorescence intensity

The change in the fluorescence intensity with bacterial concentration was measured by fluorescence spectrometry. Following centrifugation and washing with PBS buffer, the bacterial suspension was diluted with PBS to $2*10^9$ CFU mL^{-1} and subsequently diluted using a gradient method. Equal volumes of bacteria in PBS was mixed with 0.2 mg mL^{-1} of P4VP-ManTPE or P4VP-BPTPE in PBS, incubated for 2 h at 37 °C.

Hemolysis assay

Fresh sheep blood was centrifuged and washed five times with normal saline. After removing supernatant, the precipitated red blood cells were diluted to 8 vol% with PBS. Equal volumes of P4VP-ManTPE and P4VP-BPTPE at different concentrations in PBS were mixed with the red blood cell suspension. The mixture was centrifuged and the supernatant was taken to read the OD_{570} following incubation for 1 h at 37 °C. The samples with 1% Triton and PBS instead of PILs solution were positive and negative controls respectively. The formula of hemolysis rate was:

$$\text{Hemolysis rate } (\%) = \frac{\text{OD}_{\text{sample}} - \text{OD}_{\text{negative control}}}{\text{OD}_{\text{positive control}} - \text{OD}_{\text{negative control}}} \times 100\%$$

where OD was read by microplate reader under 570 nm.

Results and discussion

Synthesis and characterization of the AIE glycopolymers

Scheme 2. Synthesis route to AIE glycopolymers.

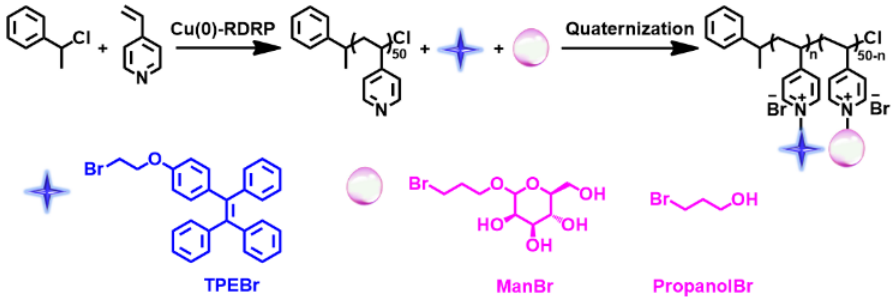

As shown in Scheme 2, copper (0) mediated reversible-deactivation radical polymerization (Cu(0)-RDRP) was employed to directly polymerize 4-vinylpyridine (4VP) at ambient temperature in DMSO / H_2O mixture (v/v = 1:1) to obtain poly(4-vinylpyridine) (P4VP) at high conversion (94%).[30] The SEC elution trace (Figure 1A) of the final P4VP revealed relatively low dispersity (M_w / M_n = 1.21, M_n = 12400 Da).

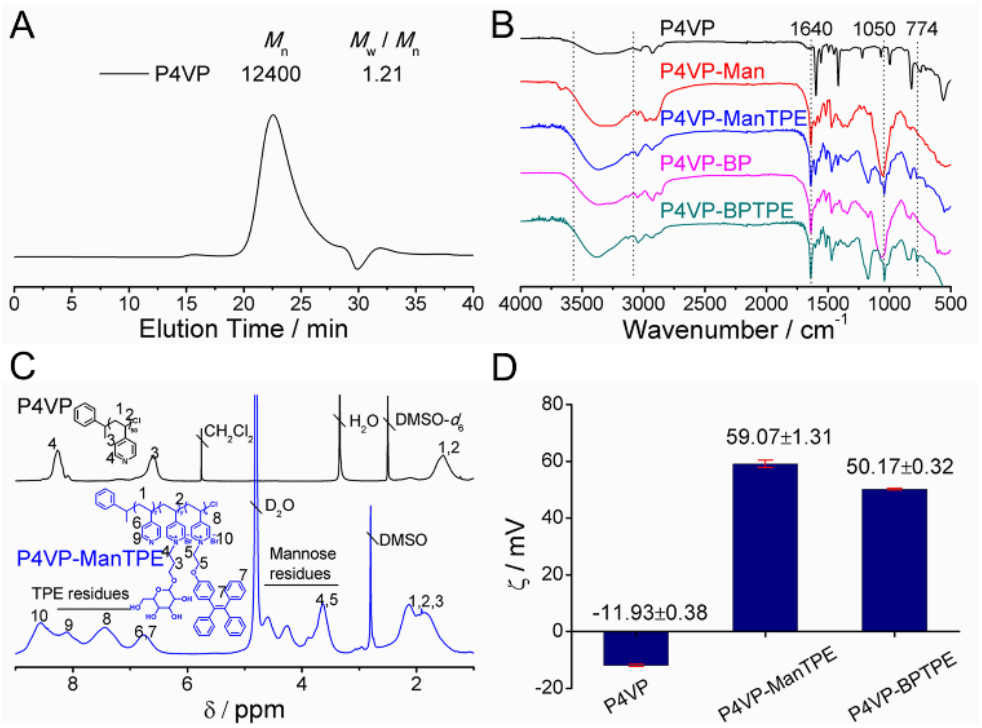

Figure 1. (A) SEC elution trace of P4VP, eluent = DMF with DRI detection. (B) FTIR spectra of P4VP and its quaternized products. (C) ^{1}H NMR (500 MHz, DMSO-d_6 / D_2O) spectra of P4VP and P4VP-ManTPE. (D) Zeta potentials (ζ) of P4VP, P4VP-ManTPE and P4VP-BPTPE.

Subsequently, quaternization reaction was used to modify P4VP with organobromine compounds such as bromine-functionalized tetraphenylethylene (TPEBr), bromine-functionalized D-mannose (ManBr) or 3-bromo-1-propanol (PropanolBr), which yielded corresponding PILs, P4VP-ManTPE and P4VP-BPTPE. As control experiments, PILs (P4VP-Man and P4VP-TPE) were synthesized in similar way without the addition of TPEBr or ManBr.

FTIR, ^{1}H NMR and ^{13}C NMR spectra could indicate the success of quaternization. In FTIR spectra (Figure 1B), the strong absorbance at 3200 ~ 3600 cm^{-1} and 1050 cm^{-1} was from hydroxyl and methylene groups of ManBr and PropanolBr, and the absorbance at 774 cm^{-1} was from benzene ring of TPE. In the spectra of quaternization products, the vibration of pyridine salts appeared at 1640 cm^{-1} and the stretching vibration of C=N at 1600 cm^{-1} almost disappeared, which indicated the success of quaternization reaction. As shown in the ^{1}H NMR spectra of P4VP (Figure 1C), the peak of polymer skeleton was shown at 1.2 ~ 1.8 ppm and peaks of pyridine appeared at 6.6 ppm and 8.3 ppm. In the spectra of P4VP-ManTPE, peaks around 3.5 ~ 4.7 ppm were from mannose residues. The characteristic peaks of TPE residues overlapped with other peaks at 6.5 ~ 8.1 ppm; however, the integral at 4.2 and 6.7 ppm of P4VP-BPTPE increased compared with that of P4VP-BP, which indicated the existence of TPE (Figure S1). The ^{13}C NMR spectra of P4VP-ManTPE (Figure S2) also

showed the resonances from quaternized 4VP as well as pendant mannose and TPE units. The ζ potentials (Figure 1D) were 59.07 mV and 50.17 mV for P4VP-ManTPE and P4VP-BPTPE, respectively, while the P4VP was negatively charged (-11.93 mV), which indicated the positive charge due to the successful quaternization.

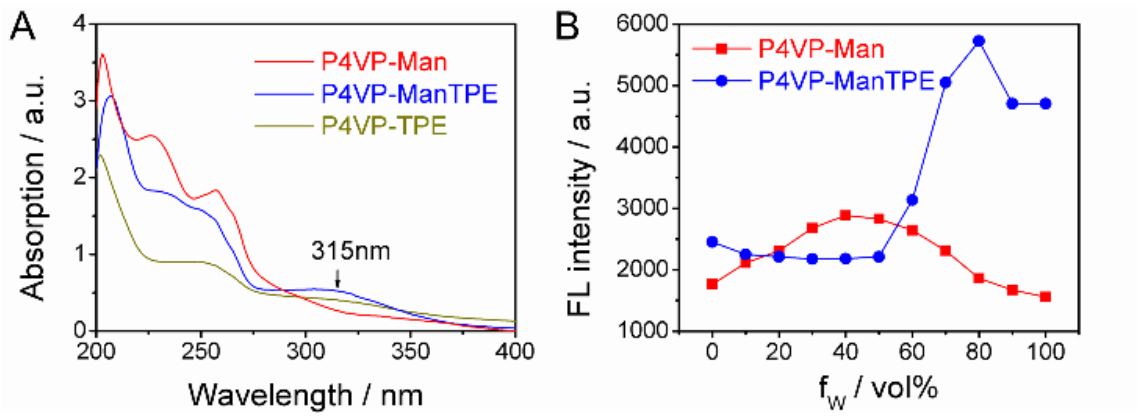

Figure 2. (A) UV-vis absorption spectra of P4VP-Man, P4VP-ManTPE and P4VP-TPE [0.1 mg mL^{-1} in MeOH / H_2O (v/v = 1:1)]; (B) Fluorescence intensity of P4VP-Man and P4VP-ManTPE in mixtures of H_2O and MeOH with different water fractions (f_W). Concentration: 0.1 mg mL^{-1}; excitation wavelength: λ = 380 nm.

Subsequently, PILs (0.1 mg mL^{-1}) in a mixture of MeOH / H_2O (v/v = 1:1) was measured by ultraviolet spectrophotometer to get relative UV-vis absorption spectra (Figure 2A). The absorption peaks of P4VP-Man appeared at 202, 226 and 258 nm. Compared with it, P4VP-TPE revealed a new absorption peak at λ = 315 nm, which was characteristic of TPE. This peak also appeared at the UV absorption spectra of P4VP-ManTPE, which further confirmed that pendant TPE was successfully introduced into polymer by quaternization reaction. The fluorescence properties of the synthesized P4VP-ManTPE and P4VP-Man dissolved in mixed MeOH / H_2O solvent were investigated by fluorescence spectrophotometer with excitation wavelength at 380 nm. In Figure 2B, fluorescence

intensity of P4VP-ManTPE gradually increased to the maximum with the increase of water fraction (f_W) from 0% to 80%, which was caused by the fact that water was the poor solvent for TPE and P4VP-ManTPE aggregated gradually with the increase of water. However, when f_W > 80%, the fluorescence intensity began to decreased, which was due to the decrease of P4VP-ManTPE's effective concentration in this poor solvent. Interestingly, P4VP-Man also showed weak fluorescence emission, although it didn't change significantly with the increase of f_W. This may be similar as AIE effect of natural saccharides.[44] In addition, with the increase of the mixed solution's polarity, the emission peak of P4VP-ManTPE appears blue shift (Figure S3). The relative quantum yields of P4VP-ManTPE and P4VP-BPTPE aqueous solutions were 0.69% and 0.97% respectively with quinine sulphate as a standard, indicating the relatively low fluorescence when dissolved. Unfortunately, the absolute quantum yields of P4VP-ManTPE and P4VP-BPTPE powders at solid state, which was measured by FLS980 series of fluorescence spectrometers, cannot be adopted due to the interference of the black colour of polymer itself and the low content of TPE.

Carbohydrate-protein recognition between PILs and ConA

As various glycoproteins such as lectins are found on the surface of many cells, it was our hypothesis that the lectin-glycopolymer interaction may help the glycopolymers identify bacteria better.[45] Therefore, the interactions between sugar-containing PILs and lectins was verified with Concanavalin A (ConA) as the model lectin. When ConA bound with PILs, the turbidity of mixture would increase, which could be observed by measuring UV absorbance at 420 nm. In the first 10 minutes, the UV absorbance of the mixed P4VP-ManTPE (2 mg mL^{-1}) and ConA (0.5 mg mL^{-1}) increased obviously, then gradually reached an equilibration.

However, the parallel P4VP-BPTPE group didn't change significantly (Figure 3A). This difference was due to the increase of turbidity caused by the aggregation of sugar-containing PILs and ConA. It is worth noting that this kind of aggregation also enhanced the fluorescence emission. When compared with P4VP-BPTPE, the fluorescence intensity of P4VP-ManTPE increased significantly after binding with ConA (Figure 3B). These results demonstrated that the sugar-containing PILs can recognize lectins as typical glycopolymers.

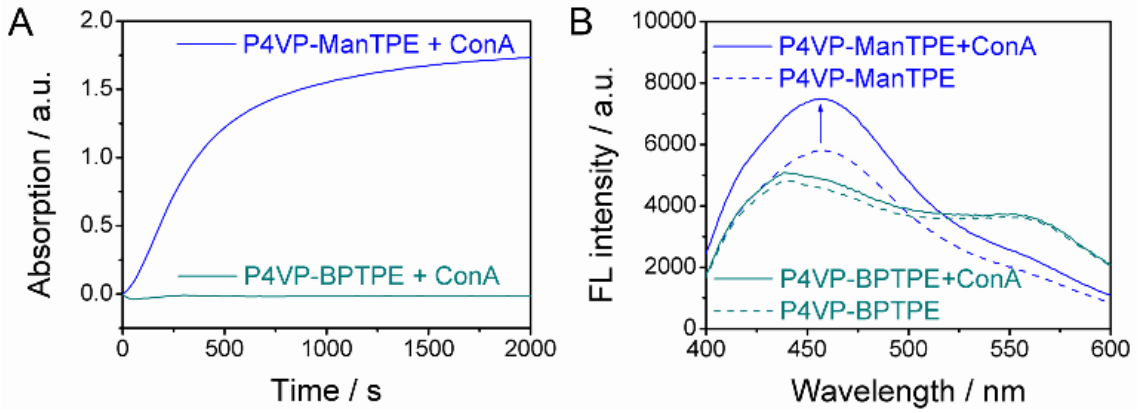

Figure 3. (A) Absorbance curve of the P4VP-ManTPE and P4VP-BPTPE mixed with ConA at λ = 420 nm. (B) Fluorescence emission spectra of P4VP-ManTPE and P4VP-BPTPE before and after addition of ConA (excitation wavelength: λ = 380 nm).

In vitro antibacterial properties of AIE PILs

Gram-positive *S. aureus* and gram-negative *E. coli* were used to investigate the antibacterial properties of the synthesized AIE PILs. Firstly, minimum inhibitory concentration (MIC) method was carried out to evaluate the antibacterial effect of P4VP-ManTPE and P4VP-BPTPE. The samples with different concentrations were prepared by 2-fold dilutions and incubated with bacterium at 37 °C for 24 h to obtain the MIC for the bacteria. Both P4VP-ManTPE and P4VP-BPTPE had better antibacterial ability on *S. aureus* than *E. coli*, which was due to the fact that gram-negative bacteria have an outer membrane to

protect the cell from being destroyed (Table 1).[46]

Table 1. Antibacterial properties of P4VP-ManTPE and P4VP-BPTPE measured as MIC.

Sample	MIC (μg mL^{-1}) for	
	E. coli	*S. aureus*
P4VP-ManTPE	1000	15.63
P4VP-BPTPE	500	7.81

The PILs bound bacteria by electrostatic interaction between cationic pyridine rings and negatively charged bacterial membranes, while the hydrophobic sections may insert into hydrophobic part of membranes to kill bacteria. Contrary to our prediction, the antibacterial effect of P4VP-BPTPE was slightly better than that of P4VP-ManTPE, which may be due to the fact that bromopropanol is more hydrophobic than mannose and is more likely to destroy the hydrophobic bacterial membranes.

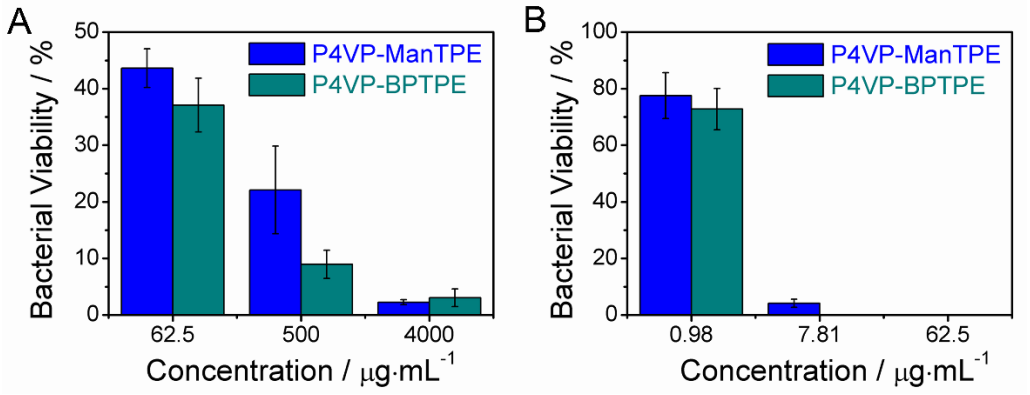

Figure 4. Bacterial viability of (A) *E. coli* and (B) *S. aureus* contacting P4VP-ManTPE and P4VP-BPTPE for 1.5 h.

Moreover, the plate count method was also carried out to verify the antibacterial ability of the PILs. The samples under corresponding concentrations (P4VP-ManTPE for 62.50, 500 and 4000 μg mL^{-1}; P4VP-BPTPE for 0.98, 7.81 and 62.50 μg mL^{-1}) were cultured with

bacteria (OD_{600} = 1 and further diluted 5000 times) at 37 °C for 1.5 h, followed by 5 μL of bacterial suspension coated on LB agar plates. The results shown in Figure 4 and Figure S4 also indicated their bactericidal effects, and the effect of P4VP-BPTPE was slightly better.

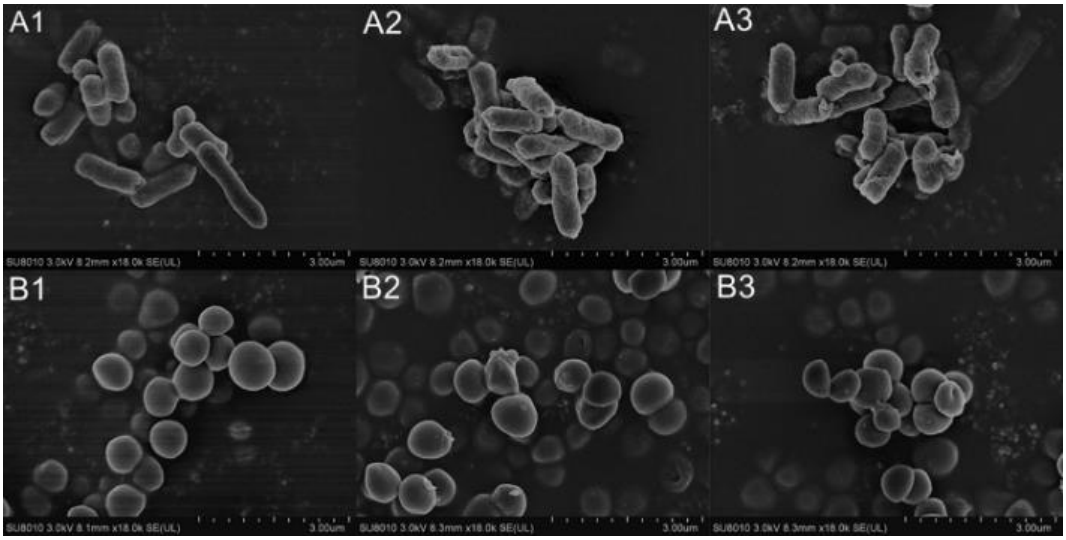

Figure 5. SEM images of *E. coli* (A1-A3) and *S. aureus* (B1-B3) co-cultured with P4VP-ManTPE (A2, B2) and P4VP-BPTPE (A3, B3) solution (0.1 mg mL^{-1}) for 2 h. Bacteria incubated without any polymers were used as control (A1, B1) (scale bar = 3 μm).

The microbial morphology of *E. coli* and *S. aureus* after incubated in PILs solution for 2 h were characterized by SEM images (Figure 5).Their partial enlarged drawings were shown in Figure S5. The bacteria in control groups (cultured without polymers) had complete morphology and smooth surface (A1, B1), while the structure of bacteria cultured with P4VP-ManTPE (A2, B2) and P4VP-BPTPE (A3, B3) were found to be partially distorted and collapsed, which indicated the occurrence of membrane damage (especially for *E. coli*) by the quanternized PILs.

Bacterial imaging and concentration detection by AIE polymers

The successful introduction of AIE probes through the quaternization reaction made it possible for the fluorescent imaging of bacteria. Both *E. coli* (A1-A3, B1-B3) and *S. aureus*

(C1-C3, D1-D3) emitted strong blue fluorescence after co-cultured with 0.1 mg mL^{-1} P4VP-ManTPE (A1-A3, C1-C3) and P4VP-BPTPE (B1-B3, D1-D3) for 2 h (Figure 6). This is due to the phenomenon that the cationic polymer accumulates on the surface of the bacteria by electrostatic and hydrophobic interactions to aggregate TPE groups and enhance fluorescence emission. It is noted that even under the same concentrations, the presence of AIE glycopolymers (P4VP-ManTPE) would stain more *E. coli* and *S. aureus* and hence made the images brighter than that of P4VP-BPTPE. This may be due to the fact that P4VP-BPTPE has only electrostatic effect on bacteria, while P4VP-ManTPE can also bind to the glycoproteins on the surface of bacteria through carbohydrate-protein recognition, which thus proved that interactions between AIE glycopolymers and bacteria. It should also be reminded that as fluorescent reagents, P4VP-ManTPE and P4VP-BPTPE were photostable, which can retain their fluorescence effect for several days without avoiding light (Figure S6).

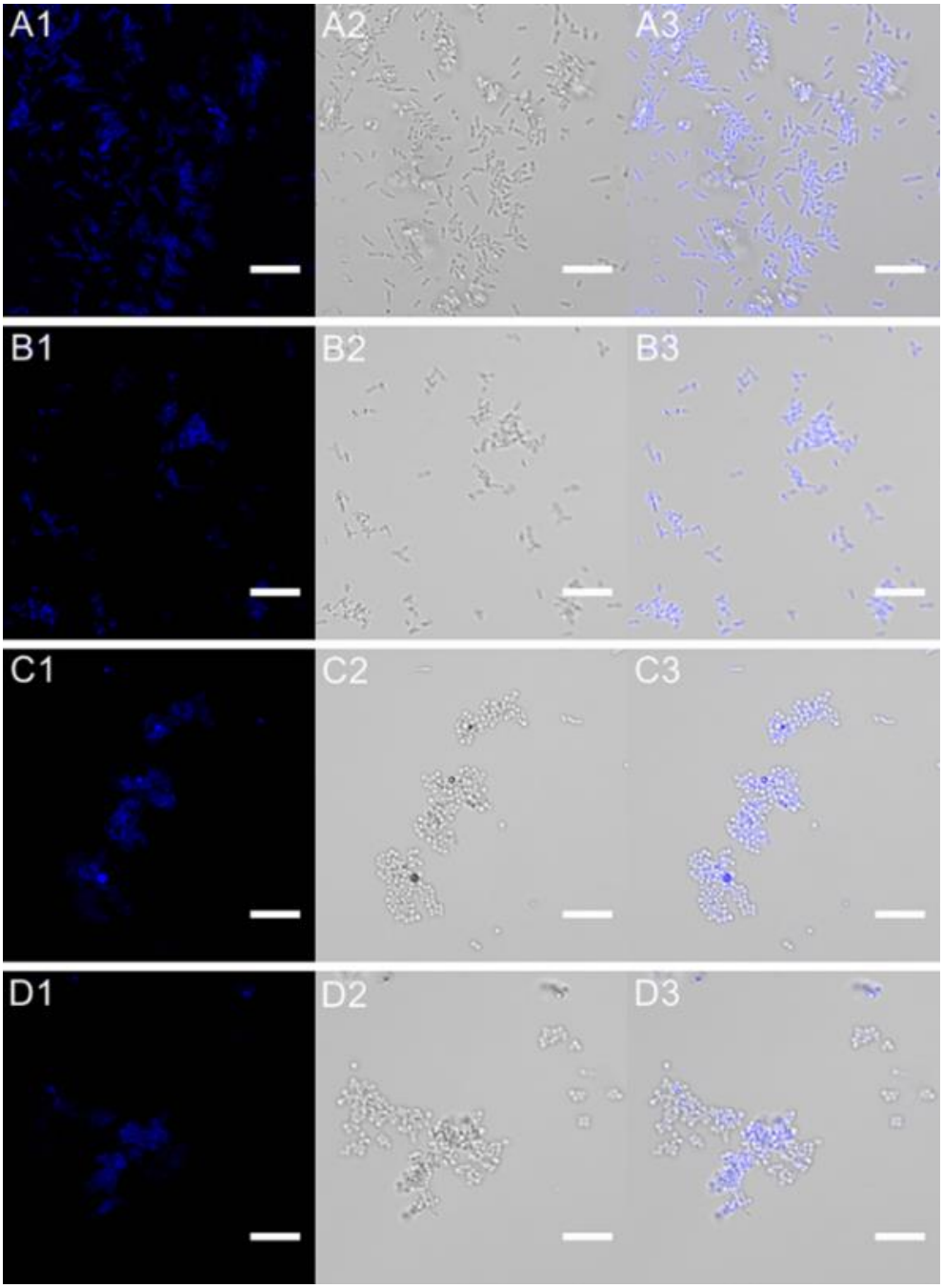

Figure 6. Fluorescence (A1-D1), bright-field (A2-D2) and superimposed (A3-D3) images of *E. coli* (A1-A3, B1-B3) and *S. aureus* (C1-C3, D1-D3) incubated with P4VP-ManTPE (A1-A3, C1-C3) and P4VP-BPTPE (B1-B3, D1-D3) (concentration: 0.1 mg mL^{-1}) for 2 h. Excitation wavelength: 300-400 nm, scale bar: 10 μm.

The relationship between bacterial concentration and fluorescence intensity was measured by fluorescence spectrometer. 0.1 mg mL^{-1} P4VP-ManTPE and P4VP-BPTPE were

co-cultured with gradient diluted bacterial suspension for 2 h in phosphate buffer (PBS), and the fluorescence spectra of the mixtures were determined at λ = 380 nm. When *E. coli* mixed with P4VP-ManTPE is taken as an example (Figure 7A), the fluorescence intensity was gradually strengthened with the increase in bacterial concentration, as bacterium accumulate more PILs on their surfaces, limiting the intramolecular rotation of TPE. The results of detecting *S. aureus* by P4VP-ManTPE and detecting *E. coli* and *S. aureus* by P4VP-BPTPE were displayed in Figure S7, S8 and S9, respectively, and the trend of fluorescence intensity summarized in Figure 7B. In general, the fluorescence intensity of P4VP-ManTPE and P4VP-BPTPE will be enhanced with the increase of bacterial concentration, which grows almost exponentially over the bacterial concentration. The response is more sensitive at relatively high concentration.

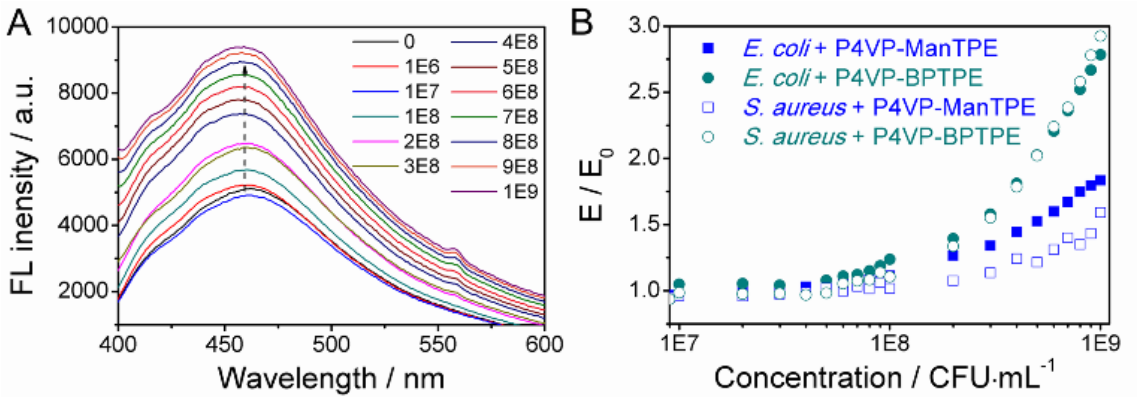

Figure 7. (A) Fluorescence spectra of 0.1 mg mL^{-1} P4VP-ManTPE mixed with different concentrations of *E. coli* in PBS (excitation wavelength: 380 nm). (B) Fluorescence intensity curves of P4VP-ManTPE (blue) and P4VP-BPTPE (green) with the concentration of *E. coli* (solid) and *S. aureus* (open). E_0: fluorescence intensity of 0.1 mg mL^{-1} PILs in PBS without bacteria; E: fluorescence intensity of 0.1 mg mL^{-1} PILs in PBS with the corresponding concentration bacteria (emission wavelength: 460 nm).

Biocompatibility evaluated by hemolysis assay

Finally, the biocompatibility of P4VP-ManTPE and P4VP-BPTPE was assessed by examining hemolytic effect of red blood cells. We found that the hemolysis rate of P4VP-ManTPE was much lower than that of P4VP-BPTPE due to the existence of mannose (Table 2). Even if its concentration reached 4 mg mL^{-1} (4*MIC *E. coli*), the hemolysis rate was only 2.95%. However the hemolysis rate of P4VP-BPTPE was as high as 16.93% under the concentration of 2 mg mL^{-1} (4*MIC *E. coli*). Thus the hemolysis rate of lower than 5% allowed P4VP-ManTPE to be used for non-direct contact biomedical materials. [47] This result proved that the presence of saccharide units can improve biocompatibility of materials.

Table 2. Hemolysis rates of P4VP-ManTPE and P4VP-BPTPE toward red blood cells.

P4VP-ManTPE		P4VP-BPTPE	
Concentration (μg mL^{-1})	Hemolysis rate (%)	Concentration (μg mL^{-1})	Hemolysis rate (%)
4000 (4*MIC *E. coli*)	2.95	/	/
2000 (2*MIC *E. coli*)	2.26	2000 (4*MIC *E. coli*)	16.93
1000 (1*MIC *E. coli*)	1.76	1000 (2*MIC *E. coli*)	7.23
/	/	500 (1*MIC *E. coli*)	3.52
62.50 (4*MIC *S. aureus*)	0.94	/	/
31.25 (2*MIC *S. aureus*)	0.82	31.25 (4*MIC *S. aureus*)	2.80
15.63 (1*MIC *S. aureus*)	0.42	15.63 (2*MIC *S. aureus*)	2.15
/	/	7.81 (1*MIC *S. aureus*)	0.58

Conclusion

In conclusion, we have successfully synthesized cationic glycopolymers with AIE effect by Cu(0)-RDRP following a facile quaternization reaction. This kind of novel fluorescent glycopolymer can be adsorbed onto bacterial surface by electrostatic non-covalent

interactions and sugar-agglutinin reaction, so as to be able to kill, image and detect bacteria. Owing to the outer membrane of gram-negative bacteria, the cationic polymers have better bactericidal effect on gram-positive bacteria. ConA has been used as a model to verify the recognition between glycopolymers and proteins. Such recognition induces the aggregation of TPE units and leads to the significant AIE effect. Compared with bromopropanol-containing PILs, mannose units in polymers could reduce the toxicity to red blood cells. When the concentration of bacteria was detected by fluorescence intensity, the response was more sensitive with the increase of bacterial concentration. The combination of antibacterial properties, imaging and low hemolysis makes the AIE glycopolymer as a useful material in the domain of biology, medicine and environmental monitoring. It is our dream to synthesize glycopolymers with precisely designed sugar code in order to recognize specific bacteria, which may help us to identify harmful or beneficial bacteria for selective killing.

ASSOCIATED CONTENT

Supporting Information.

The Supporting Information is available free of charge on the ACS Publications website. ^{1}H NMR of PILs, ^{13}C of P4VP-ManTPE, fluorescence emission spectra of P4VP-ManTPE in MeOH / H_2O, LB agar plates of incubated bacteria with P4VP-ManTPE and P4VP-BPTPE and fluorescence spectra of PILs mixed with bactria (PDF).

AUTHOR INFORMATION

Corresponding Author

* E-mail: zhangqiang@njust.edu.cn (Qiang Zhang).

* E-mail: d.m.haddleton@warwick.ac.uk (David M. Haddleton).

ORCID

Qiang Zhang: 0000-0003-4596-9993

David M. Haddleton: 0000-0002-4965-0827

Notes

The authors declare no competing financial interest.

ACKNOWLEDGMENT

This project was conducted with financial support from the Natural Science Foundation of Jiangsu Province for Distinguished Young Scholars (BK20180017), Sichuan Science and Technology Program (2020YFSY0028) and the Research Project of the Education Department of Sichuan Province, China (17ZA0370).

REFERENCES

1. Jain, A.; Duvvuri, L. S.; Farah, S.; Beyth, N.; Domb, A. J.; Khan, W., Antimicrobial Polymers. *Adv. Healthc. Mater.* **2014,** 3, (12), 1969-1985.
2. Dong, Y. S.; Xiong, X. H.; Lu, X. W.; Wu, Z. Q.; Chen, H., Antibacterial surfaces based on poly(cationic liquid) brushes: switchability between killing and releasing via anion counterion switching. *J. Mat. Chem. B* **2016,** 4, (36), 6111-6116.
3. Lode, H. M., Clinical impact of antibiotic-resistant Gram-positive pathogens. *Clin. Microbiol. Infect.* **2009,** 15, (3), 212-217.
4. Rizzello, L.; Pompa, P. P., Nanosilver-based antibacterial drugs and devices: Mechanisms, methodological drawbacks, and guidelines. *Chem. Soc. Rev.* **2014,** 43, (5), 1501-1518.
5. Krizsan, A.; Volke, D.; Weinert, S.; Strater, N.; Knappe, D.; Hoffmann, R., Insect-Derived Proline-Rich Antimicrobial Peptides Kill Bacteria by Inhibiting Bacterial Protein Translation at the 70S Ribosome. *Angew. Chem.-Int. Edit.* **2014,** 53, (45), 12236-12239.
6. Delezuk, J. A. M.; Ramirez-Herrera, D. E.; de Avila, B. E. F.; Wang, J., Chitosan-based water-propelled micromotors with strong antibacterial activity. *Nanoscale* **2017,** 9, (6), 2195-2200.
7. Lipovsky, A.; Thallinger, B.; Perelshtein, I.; Ludwig, R.; Sygmund, C.; Nyanhongo, G. S.; Guebitz, G. M.; Gedanken, A., Ultrasound coating of polydimethylsiloxanes with

antimicrobial enzymes. *J. Mat. Chem. B* **2015,** 3, (35), 7014-7019.
8. Egorova, K. S.; Gordeev, E. G.; Ananikov, V. P., Biological Activity of Ionic Liquids and Their Application in Pharmaceutics and Medicine. *Chem. Rev.* **2017,** 117, (10), 7132-7189.
9. Lu, Z.; Zhang, X.; Li, Z.; Wu, Z.; Song, J.; Li, C., Composite copolymer hybrid silver nanoparticles: preparation and characterization of antibacterial activity and cytotoxicity. *Polym. Chem.* **2015,** 6, (5), 772-779.
10. Krishnamoorthy, K.; Veerapandian, M.; Zhang, L.-H.; Yun, K.; Kim, S. J., Antibacterial Efficiency of Graphene Nanosheets against Pathogenic Bacteria via Lipid Peroxidation. *J. Phys. Chem. C* **2012,** 116, (32), 17280-17287.
11. Ng, Y. H.; Ikeda, S.; Matsumura, M.; Amal, R., A perspective on fabricating carbon-based nanomaterials by photocatalysis and their applications. *Energy Environ. Sci.* **2012,** 5, (11), 9307-9318.
12. Guo, J. N.; Qin, J.; Ren, Y. Y.; Wang, B.; Cui, H. Q.; Ding, Y. Y.; Mao, H. L.; Yan, F., Antibacterial activity of cationic polymers: side-chain or main-chain type? *Polym. Chem.* **2018,** 9, (37), 4611-4616.
13. Yuan, H. M.; Yu, B. R.; Fan, L. H.; Wang, M.; Zhu, Y. W.; Ding, X. K.; Xu, F. J., Multiple types of hydroxyl-rich cationic derivatives of PGMA for broad-spectrum antibacterial and antifouling coatings. *Polym. Chem.* **2016,** 7, (36), 5709-5718.
14. Mazrad, Z. A. I.; In, I.; Lee, K. D.; Park, S. Y., Rapid fluorometric bacteria detection assay and photothermal effect by fluorescent polymer of coated surfaces and aqueous state. *Biosens. Bioelectron.* **2017,** 89, 1026-1033.
15. Chen, J.; Wang, F.; Liu, Q.; Du, J., Antibacterial polymeric nanostructures for biomedical applications. *Chem. Commun.* **2014,** 50, (93), 14482-14493.
16. Li, X.; Bai, H. T.; Yang, Y. C.; Yoon, J.; Wang, S.; Zhang, X., Supramolecular Antibacterial Materials for Combatting Antibiotic Resistance. *Adv. Mater.* **2019,** 31, (5), 1805092.
17. Rauner, N.; Mueller, C.; Ring, S.; Boehle, S.; Strassburg, A.; Schoeneweiss, C.; Wasner, M.; Tiller, J. C., A Coating that Combines Lotus-Effect and Contact-Active Antimicrobial Properties on Silicone. *Adv. Funct. Mater*. **2018,** 28, (29), 1801248.
18. Xue, Y.; Pan, Y.; Xiao, H.; Zhao, Y., Novel quaternary phosphonium-type cationic polyacrylamide and elucidation of dual-functional antibacterial/antiviral activity. *RSC Adv.* **2014,** 4, (87), 46887-46895.
19. Fang, C.; Kong, L.; Ge, Q.; Zhang, W.; Zhou, X.; Zhang, L.; Wang, X., Antibacterial activities of N-alkyl imidazolium-based poly(ionic liquid) nanoparticles. *Polym. Chem.* **2019,** 10, (2), 209-218.
20. Sundararaman, M.; Rajesh Kumar, R.; Venkatesan, P.; Ilangovan, A., 1-Alkyl-(N,N-dimethylamino)pyridinium bromides: inhibitory effect on virulence factors of Candida albicans and on the growth of bacterial pathogens. *J. Med. Microbiol.* **2013,** 62, (2), 241-248.
21. Iwai, N.; Nakayama, K.; Kitazume, T., Antibacterial activities of imidazolium, pyrrolidinium and piperidinium salts. *Bioorg. Med. Chem. Lett.* **2011,** 21, (6), 1728-1730.
22. Qin, J.; Guo, J.; Xu, Q.; Zheng, Z.; Mao, H.; Yan, F., Synthesis of Pyrrolidinium-Type Poly(ionic liquid) Membranes for Antibacterial Applications. *ACS Appl. Mater. Interfaces* **2017,** 9, (12), 10504-10511.

23. Xue, H.; Zhao, Z.; Chen, S.; Du, H.; Chen, R.; Brash, J. L.; Chen, H., Antibacterial coatings based on microgels containing quaternary ammonium ions: Modification with polymeric sugars for improved cytocompatibility. *Colloid Interface Sci. Commun.* **2020,** 37, 100268.
24. Liu, M.; Wang, K.; Zhang, X.; Zhang, X.; Li, Z.; Zhang, Q.; Huang, Z.; Wei, Y., Fabrication of stable and biocompatible red fluorescent glycopolymer nanoparticles for cellular imaging. *Tetrahedron* **2015,** 71, (34), 5452-5457.
25. Liu, W.; Chaix, A.; Gary-Bobo, M.; Angeletti, B.; Masion, A.; Da Silva, A.; Daurat, M.; Lichon, L.; Garcia, M.; Morere, A.; El Cheikh, K.; Durand, J. O.; Cunin, F.; Auffan, M., Stealth Biocompatible Si-Based Nanoparticles for Biomedical Applications. *Nanomaterials* **2017,** 7, (10), 288.
26. Hong, M.; Miao, Z.; Xu, X.; Zhang, Q., Magnetic Iron Oxide Nanoparticles Immobilized with Sugar-Containing Poly(ionic liquid) Brushes for Efficient Trapping and Killing of Bacteria. *ACS Appl. Bio Mater.* **2020,** 3, (6), 3664-3672.
27. Liu, M.; Li, J.; Li, B., Mannose-Modificated Polyethylenimine: A Specific and Effective Antibacterial Agent against Escherichia coli. *Langmuir* **2018,** 34, (4), 1574-1580.
28. Miao, Z.; Li, D.; Zheng, Z.; Zhang, Q., Synthesis of chitosan-mimicking cationic glycopolymers by Cu(0)-LRP for efficient capture and killing of bacteria. *Polym. Chem.* **2019,** 10, (29), 4059-4066.
29. Cuthbert, T. J.; Hisey, B.; Harrison, T. D.; Trant, J. F.; Gillies, E. R.; Ragogna, P. J., Surprising Antibacterial Activity and Selectivity of Hydrophilic Polyphosphoniums Featuring Sugar and Hydroxy Substituents. *Angew. Chem., Int. Ed.* **2018,** 57, (39), 12707-12710.
30. Chen, J.; Li, D.; Bao, C. Y.; Zhang, Q., Controlled synthesis of sugar-containing poly(ionic liquid)s. *Chem. Commun.* **2020,** 56, (25), 3665-3668.
31. Zhao, E. G.; Hong, Y. N.; Chen, S. J.; Leung, C. W. T.; Chan, C. Y. K.; Kwok, R. T. K.; Lam, J. W. Y.; Tang, B. Z., Highly Fluorescent and Photostable Probe for Long-Term Bacterial Viability Assay Based on Aggregation-Induced Emission. *Adv. Healthc. Mater.* **2014,** 3, (1), 88-96.
32. Naik, V. G.; Hiremath, S. D.; Das, A.; Banwari, D.; Gawas, R. U.; Biswas, M.; Banerjee, M.; Chatterjee, A., Sulfonate-functionalized tetraphenylethylenes for selective detection and wash-free imaging of Gram-positive bacteria (Staphylococcus aureus). *Mater. Chem. Front.* **2018,** 2, (11), 2091-2097.
33. Shi, J.; Wang, M.; Sun, Z.; Liu, Y.; Guo, J.; Mao, H.; Yan, F., Aggregation-induced emission-based ionic liquids for bacterial killing, imaging, cell labeling, and bacterial detection in blood cells. *Acta Biomater.* **2019,** 97, 247-259.
34. Tang, B. Z.; Zhan, X.; Yu, G.; Sze Lee, P. P.; Liu, Y.; Zhu, D., Efficient blue emission from siloles. *J. Mater. Chem.* **2001,** 11, (12), 2974-2978.
35. Li, D.; Chen, J.; Xu, X.; Bao, C.; Zhang, Q., Supramolecular assemblies of glycoclusters with aggregation-induced emission for sensitive phenol detection. *Chem. Commun.* **2020,** 56, (87), 13385-13388.
36. Wang, M.; Zhang, G.; Zhang, D.; Zhu, D.; Tang, B. Z., Fluorescent bio/chemosensors based on silole and tetraphenylethene luminogens with aggregation-induced emission feature. *J. Mater. Chem.* **2010,** 20, (10), 1858-1867.
37. Dong, Y.; Lam, J. W. Y.; Qin, A.; Liu, J.; Li, Z.; Tang, B. Z.; Sun, J.; Kwok, H. S.,

Aggregation-induced emissions of tetraphenylethene derivatives and their utilities as chemical vapor sensors and in organic light-emitting diodes. *Appl. Phys. Lett.* **2007,** 91, (1), 011111.
38. Wang, M. Y.; Shi, J.; Mao, H. L.; Sun, Z.; Guo, S. Y.; Guo, J. N.; An, F., Fluorescent Imidazolium-Type Poly(ionic liquid)s for Bacterial Imaging and Biofilm Inhibition. *Biomacromolecules* **2019,** 20, (8), 3161-3170.
39. Davis, B. G.; Wood, S. D.; Maughan, M. A. T., Towards an unprotected self-activating glycosyl donor system: Bromobutyl glycosides. *Can. J. Chem.* **2002,** 80, (6), 555-558.
40. Guo, Y.; Shi, D.; Luo, Z. W.; Xu, J. R.; Li, M. L.; Yang, L. H.; Yu, Z. Q.; Chen, E. Q.; Xie, H. L., High Efficiency Luminescent Liquid Crystalline Polymers Based on Aggregation-Induced Emission and "Jacketing" Effect: Design, Synthesis, Photophysical Property, and Phase Structure. *Macromolecules* **2017,** 50, (24), 9607-9616.
41. Li, Y.; Song, C.; Wang, Y.; Wei, Y.; Wei, Y.; Hu, Y., High photoluminescence quantum yield of TiO2 nanocrystals prepared using an alcohothermal method. *Luminescence* **2007,** 22, (6), 540-545.
42. Cairo, C. W.; Gestwicki, J. E.; Kanai, M.; Kiessling, L. L., Control of Multivalent Interactions by Binding Epitope Density. *J. Am. Chem. Soc.* **2002,** 124, (8), 1615-1619.
43. Andrews, J. M., Determination of minimum inhibitory concentrations. *J. Antimicrob. Chemother.* **2001,** 48, (suppl_1), 5-16.
44. Wang, Y.; Nie, J.; Fang, W.; Yang, L.; Hu, Q.; Wang, Z.; Sun, J. Z.; Tang, B. Z., Sugar-Based Aggregation-Induced Emission Luminogens: Design, Structures, and Applications. *Chem. Rev.* **2020,** 120, (10), 4534-4577.
45. Tsutsumi, H.; Ohkusa, H.; Park, H.; Takahashi, T.; Yuasa, H.; Mihara, H., Gold nanoparticles conjugated with monosaccharide-modified peptide for lectin detection. *Bioorg. Med. Chem. Lett.* **2012,** 22, (22), 6825-6827.
46. Sperandeo, P.; Martorana, A. M.; Polissi, A., The lipopolysaccharide transport (Lpt) machinery: A nonconventional transporter for lipopolysaccharide assembly at the outer membrane of Gram-negative bacteria. *J. Biol. Chem.* **2017,** 292, (44), 17981-17990.
47. Jordan, A. N.; Das, S.; Siraj, N.; de Rooy, S. L.; Li, M.; El-Zahab, B.; Chandler, L.; Baker, G. A.; Warner, I. M., Anion-controlled morphologies and spectral features of cyanine-based nanoGUMBOS - an improved photosensitizer. *Nanoscale* **2012,** 4, (16), 5031-5038.

Table of Contents